http://dx.doi.org/10.11142/jicems.2013.2.3.306
Journal of International Conference on Electrical Machines and Systems Vol. 2, No. 3, pp. 306~312, 2013

A New Flux Tracking LVRT Control Scheme for Doubly Fed Induction Generators

Sun-Young Park *, Hyung-Jin Ahn **, and Dong-Myung Lee **

Abstract – Doubly fed induction generator (DFIG) systems widely used globally are highly sensitive to the grid disturbance due to the structure that the stator is connected to the grid. In the past, when a grid fault occurs in order to prevent a system, generators are separated from the grid regardless of the fault duration time. Recently, however, the grid connection standards(Grid Code)says that for the failures removed within a certain time, the generator remains operation without separating from the grid. This paper proposes a new flux tracking LVRT(Low-Voltage Ride Through) control based on system modeling equations. The validity of the proposed strategy has been demonstrated by computer simulations.

Keywords: LVRT, DFIG system, Voltage dips, Flux tracking, Grid faults

1. Introduction

Recently, wind energy generation is attracting attentions globally. It is considered as the eco generation due to generating electric powers from physical energy of winds. The depletion of fossil fuels and environmental pollution increase the interest in the renewable energy such as wind power. In the last 20 years, renewable energy including wind power market has been rapidly increasing in size. The report of 2012 WWEA (World Wide Energy Association) reported that total installed capacity of wind power in global reached 254GW[1]. This is the increase by 16.4% compared to 2011, and it shows that wind power market continues its upward trend.

In case of Korea, large offshore wind park is expected to be constructed in Jeju-island, and the development plan of green-island using new renewable energy technology including wind power energy has been scheduled in Ulleung-island chosen as green energy test site. As wind power energy is increasing its interests and demand, grid connection, grid control, and stability assurance technology of a generating systemare emerged as an important research project for national competitiveness.

Depending on the structure, wind energy generation system can be classified into four types [2]. DFIG (Doubly Fed Induction Generator) systems with type 3, which have been adopted widely by world's leading wind turbine manufacturing companies, consist of back-to-back PWM converters, DC-link capacitors and a wound-rotor induction machine and so on.

In the DFIG systems, the stator of the generator is connected to the gridand the rotor of it is connected to back-to-back converter. DFIG systems can maintain the constant grid frequency regardless of the variation of wind speed, and can control the generation of active and reactive power. Type 4 of wind power generation systems is defined as a wind generation system with full power rated converters [2]. In type 4, the capacity of generator is the same as that of converter. Unlike type 4, the capacity of converter in the DFIG system is about 30% of that of the generator. Thanks to these advantages, DFIG systems currently have the largest share of the market for wind energy generators.

DFIG systems are highly sensitive about grid disturbances due to the structure that the stator is connected directly to the grid. In the past, when a grid fault occurs in order to prevent a system, generators are separated from the grid. Recently, however, the grid connection standards (Grid Code) defines that for the gridfailures that last a certain time the generator remains operation without separating from the grid [3]. Thus, the wind power generation system connected to the grid should have ride-through function during grid faults as well as control of power generation during normal grid conditions. An existing LVRT (Low Voltage Ride Through) control prepares for malfunctions by using additional protective equipment such as crow-bar circuit. In order to reduce the cost of additional equipment, various techniques have been introduced [4-6]. This paper proposes a new LVRT scheme by flux tracking method done in synchronous rotating

* HAE R&D center in LG Electronics, Seoul, Korea.
** School of Electronic and Electrical Engineering, Hongik University, Seoul, Korea.
Received 12 July 2013; Accepted 20 August 2013

reference frame of induction machine based on the scheme in paper [6]. The validity of the proposed strategy is demonstrated by simulations carried out with MATLAB/SIMULINK.

2. DFIG Systems

2.1 DFIG System Modeling

In case of DFIG system modeling, most paper use stator-flux oriented reference frame. When using the stator-flux oriented reference frame, it is easy to control RSC(Rotor Side Converter), and the stator flux can be easily calculated using stator voltage and current.

In the synchronous rotating reference frame, voltage equations of stator and rotor on the d-q axis can be expressed as

$$\upsilon_{ds}^{e} = R_s i_{ds}^{e} + \frac{d}{dt}\lambda_{ds}^{e} - \omega_e \lambda_{qs}^{e} \tag{1}$$

$$\upsilon_{qs}^{e} = R_s i_{qs}^{e} + \frac{d}{dt}\lambda_{qs}^{e} + \omega_e \lambda_{ds}^{e} \tag{2}$$

$$\upsilon_{dr}^{e} = R_r i_{dr}^{e} + \frac{d}{dt}\lambda_{dr}^{e} - (\omega_e - \omega_r)\lambda_{qr}^{e} \tag{3}$$

$$\upsilon_{qr}^{e} = R_r i_{qr}^{e} + \frac{d}{dt}\lambda_{qr}^{e} + (\omega_e - \omega_r)\lambda_{dr}^{e} \tag{4}$$

where, R_s is the stator resistance, v_{dqs}^{e} is the stator voltage, i_{dqs}^{e} is the stator current, λ_{dqs}^{e} is the stator flux, υ_{dqr}^{e} is the rotor voltage, i_{dqr}^{e} is the rotor current, λ_{dqr}^{e} is the rotor flux, ω_e is synchronous angular speed, and ω_r is angular speed of the rotor. The slip angular speed ω_{sl} is expressed as

$$\omega_{sl} = \omega_e - \omega_r \tag{5}$$

The flux equations of the stator and the rotor are given by

$$\lambda_{ds}^{e} = L_s i_{ds}^{e} + L_m i_{dr}^{e} \tag{6}$$

$$\lambda_{qs}^{e} = L_s i_{qs}^{e} + L_m i_{qr}^{e} \tag{7}$$

$$\lambda_{dr}^{e} = L_m i_{ds}^{e} + L_r i_{dr}^{e} \tag{8}$$

$$\lambda_{qr}^{e} = L_m i_{qs}^{e} + L_r i_{qr}^{e} \tag{9}$$

where, L_m is the mutual inductance, L_s is the stator inductance, and L_r is the rotor inductance.

The d-q axis equivalent circuit of the DFIG system is shown in Fig. 1.

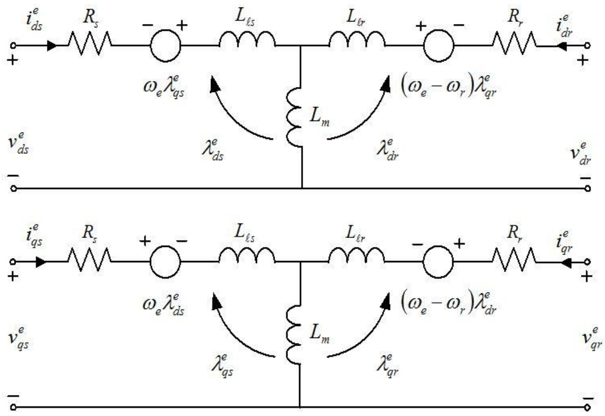

Fig. 1. The d-q axis equivalent circuit of DFIGs

To apply for stator-flux oriented control, the detection of phase angle of the stator flux is briefly explained. In the stationary reference frame, the stator voltagesare given by

$$\upsilon_{ds}^{s} = R_s i_{ds}^{s} + \frac{d}{dt}\lambda_{ds}^{s} \tag{10}$$

$$\upsilon_{qs}^{s} = R_s i_{qs}^{s} + \frac{d}{dt}\lambda_{qs}^{s} \tag{11}$$

Thus, the stator flux and the phase angle of it in the stationary reference frame are expressed as

$$\lambda_{ds}^{s} = \int (\upsilon_{ds}^{s} - R_s i_{ds}^{s})dt \tag{12}$$

$$\lambda_{qs}^{s} = \int (\upsilon_{qs}^{s} - R_s i_{qs}^{s})dt \tag{13}$$

$$\theta_e = \tan^{-1}\left(\frac{\lambda_{qs}^{s}}{\lambda_{ds}^{s}}\right) \tag{14}$$

From above equations it is noticed that the stator flux is aligned with the d-axis in the synchronous rotating reference frame. Fig. 2 shows stator fluxes in the stationary frame and its phase.

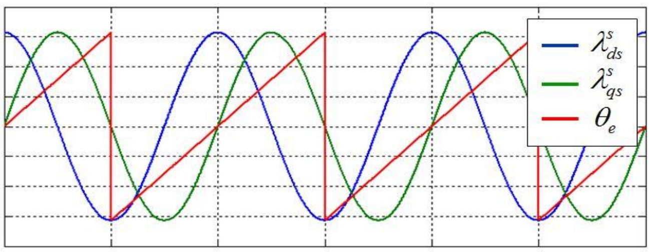

Fig. 2. The stator flux and phase angle of the stator flux

2.2 DFIG System Configuration

The overall DFIG system is shown in Fig. 3.

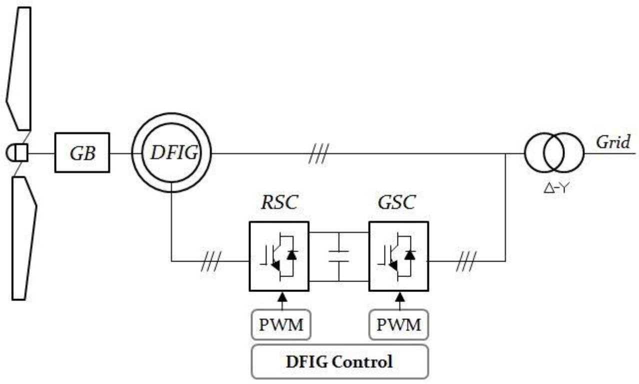

Fig. 3. The overall wind energy generation system using DFIG

The DFIG system consists of back-to-back converter, DC-link voltage and an induction machine. Back-to-back converters mean RSC and GSC(Grid-Side Converter).

2.3 DFIG System Control [7]-[8]

The DFIG control system can be divided into the control of the RSC and that of the GSC. The RSC is controlled with the stator-flux oriented vector control, and regulates the stator active power and reactive power. The stator active power and reactive power are shown as follows

$$P_s = \frac{3}{2}\left(\upsilon_{qs}^e i_{qs}^e + \upsilon_{ds}^e i_{ds}^e\right) \tag{15}$$

$$Q_s = \frac{3}{2}\left(\upsilon_{qs}^e i_{ds}^e - \upsilon_{ds}^e i_{qs}^e\right) \tag{16}$$

After expressing the stator flux, (6) and (7), as the stator current, substituting them into (15) and (16), (17) and (18) are obtained

$$P_s \approx -\frac{3}{2}\left(\frac{L_m}{L_s}\right)\upsilon_{qs}^e \upsilon_{qr}^e \tag{17}$$

$$Q_s \approx -\frac{3}{2}\left(\frac{L_m}{L_s}\right)\upsilon_{qs}^e \upsilon_{dr}^e + \frac{3}{2}\left(\frac{1}{L_s}\right)\upsilon_{qs}^e \lambda_{ds}^e \tag{18}$$

If the stator resistance is very small, the stator voltage and the stator flux have a 90° phase difference according to (10) and (11). Thus the value of υ_{ds}^e is negligible relative to that of υ_{qs}^e. Consequently, the stator active and reactive powers are approximated as (17) and (18), respectively. If feed-forward compensation is well conducted, power of the stator can be controlled independently by rotor currents. The entire control block of the RSC is shown in Fig. 4.

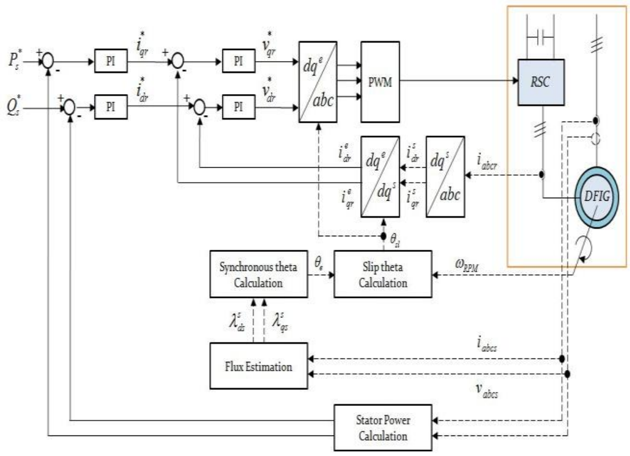

Fig. 4. The control block diagram of the rotor side converter

The GSC uses vector control with grid voltage oriented. It controls DC-link voltage and the reactive power provided to the grid. Because the RSC controls reactive power provided to a grid in general, the GSC regulates that as zero. L-filter is connected between the GSC and the grid. The configuration of a circuit between the GSC and the grid is shown in Fig. 5.

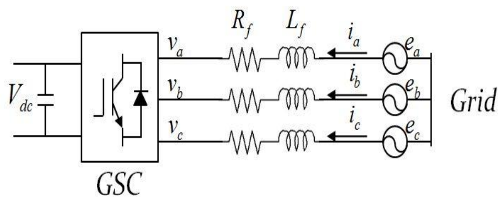

Fig. 5. Grid side converter with L-filter

The grid voltages are expressed as

$$e_a = R_f i_a + L_f \frac{d}{dt} i_a + \upsilon_a \tag{19}$$

$$e_b = R_f i_b + L_f \frac{d}{dt} i_b + \upsilon_b \tag{20}$$

$$e_c = R_f i_c + L_f \frac{d}{dt} i_c + \upsilon_c \tag{21}$$

In this paper, the grid voltage is aligned with q-axis in grid voltage oriented reference frame. If 3-phase voltage equations, (19) ~ (21), are described in synchronous rotating reference frame, those can be expressed as.

$$e_d^e = R_f i_{ds}^e + L_f \frac{d}{dt} i_{ds}^e - \omega_e L_f i_{qs}^e + \upsilon_d^e \qquad (22)$$

$$e_q^e = R_f i_{qs}^e + L_f \frac{d}{dt} i_{qs}^e - \omega_e L_f i_{qs}^e + \upsilon_q^e \qquad (23)$$

The active power and reactive powers provided from GSC are expressed as

$$P_{conv} = \frac{3}{2} e_q^e i_{qs}^e \qquad (24)$$

$$Q_{conv} = \frac{3}{2} e_d^e i_{ds}^e \qquad (25)$$

The DC-link voltage can be controlled by the q-axis current and the reactive power can be controlled by the d-axis current, as shown in (24) and (25). The entire control block of GSC is shown in Fig. 6.

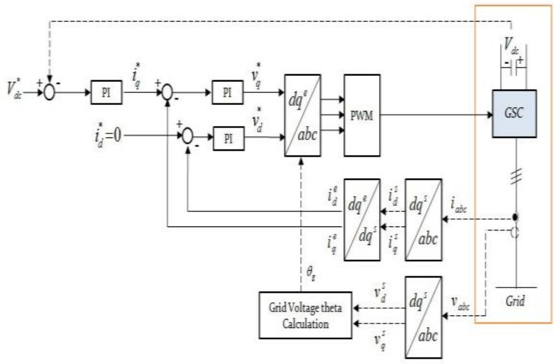

Fig. 6. Control block diagram of the GSC

3. LVRT Control Scheme

3.1 System Dynamic Characteristic under Grid Faults

This paperdeals with the control of RSC when there is a serious low voltage 3-phase balanced fault. First, if a fault occurs in the system, it has problems summarized as follows [9].

- The mechanical output (P_m) is the same as the sum of the stator power(P_s) and the rotor power(P_r) with ignoring of system losses. If a serious level of low voltage fault occurs, the stator power will rapidly be reduced. In general, as the inertia of generator is very large, the rotor speed cannot change abruptly, which means the mechanical output of wind turbine is unchanged. Hence, the rotor power is increasing as much as the reduction of the stator power consumption.

$$\begin{aligned} Normal: P_m &= P_s + P_r \\ Fault: P_m &\approx P_r \end{aligned} \qquad (26)$$

- During a fault, the sudden increase of the rotor power generates overvoltage and over-current in rotor side and changes the dynamic characteristics of system. The developed over-current and over-voltage, whose values are several times bigger than the normal levels, increase DC-link voltage and may destroy the RSC.

3.2 Existing LVRT Control Method

Existing LVRT control techniques, which protect the overvoltage and over-current in the rotor side for grid faults, such as crow-bar, ESD [10] or DVR [11] use additional protection equipment. In most systems, an additional protection equipment such as an active crow-bar circuit is installed [12]. Even such equipment is able to deal with fault reliably and immediately, it increases the cost of the system.

A typical method protecting the overvoltage and the over-current is the change of current command. For example, there are injection scheme of a current opposite to the magnetic flux, feedback technique of the stator current [5] and so on. Such techniques can reduce the cost of additional equipment, but it is essential to analyze exactly dynamic characteristics of the system. Also, it may work only in feasible region.

3.3 Proposed LVRT Control Technique

This paper proposes a new flux tracking LVRT technique using synchronous rotating reference frame based on reference [6]. Same as the idea of paper [6], to suppress over-current and over-voltage of the rotor during a grid fault, the RSC is controlled in the manner that the stator flux tracks the rotor flux. Meanwhile, a flux tracking technique proposed in paper [6] determines the level of the flux tracking depending on tracking constant k ($0 \le k \le 1$).

The command for the rotor flux is set as $k\lambda_s$ during a fault corresponding to the level of grid failure [6]. Controlling the value of k depending on the dip of low-voltage, this scheme enhances the performance of control. However, controller performance is very sensitive to tracking constant k . For a more stable controller performance, the proposed flux tracking technique determines the rotor reference currents according to the system equations and grid code instead of a tracking constant.

In case of a fault, this paper uses a command of active power and reactive power of the stator provided by the grid code instead of the value of k in paper [6], and suppresses the over-current in the rotor by tracking the rotor flux to the stator flux.

In this paper, the generation of a command can be explained as follows. After expressing stator flux, substituting (6) and (7), as the stator current, into (8) and (9), followings are obtained

$$\lambda_{dr}^e = \frac{L_m}{L_s}\lambda_{ds}^e - \sigma L_r i_{dr}^e \tag{27}$$

$$\lambda_{qr}^e = \frac{L_m}{L_s}\lambda_{qs}^e - \sigma L_r i_{qr}^e \tag{28}$$

$$where \quad \sigma = 1 - \frac{L_m^2}{L_s L_r}$$

In (27) and (28), provided $L_m / L_s \approx 1,$ the rotor currents are denoted as

$$i_{dr}^e = \frac{1}{\sigma L_r}\left(\lambda_{dr}^e - \lambda_{ds}^e\right) \tag{29}$$

$$i_{qr}^e = \frac{1}{\sigma L_r}\left(\lambda_{qr}^e - \lambda_{qs}^e\right) \tag{30}$$

From (29) and (30) it can be known that the rotor current is determined by difference between the stator flux and the rotor flux.

If the rating of the rotor is $\mathrm{I}_{r\max}$, the stator flux and the rotor flux should have the following range.

$$\lambda_{dqr}^e - \lambda_{dqs}^e \le \sigma L_r \mathrm{I}_{r\max} \tag{31}$$

When the fault occurs, in order to suppress rotor current below $\mathrm{I}_{r\max}$, the flux command is configured as the rotor flux(λ_{dqr}^e) tracks the stator flux(λ_{dqs}^e). When a fault occurs, the command of rotor current can be selected as zero or the value according to level of voltage dip to satisfy the grid code.

In this paper, under the assumption that the wind velocity and generator speed don't have big changes before and after a fault, the rotor flux command is configured to maintain the rotor current level as that before the fault occurs. Meanwhile, active power is controlled by i_{qr}^e as known from (28) as

$$\lambda_{qr}^* = \lambda_{qs}^e + \sigma L_r I_{qr_{steasy-state}}^e \tag{32}$$

In case of reactive power, depending on the grid code of each country, the rotor flux command is given with consideration of a low-voltage dip. Grid code of Germany and Spain concerning about reactive power is shown in Fig. 7. In the grid code of Germany, if the grid voltage is below its 50% nominal value, the rotor current command of reactive power is set as -1 [p.u.]. In this proposed scheme, the command of i_{dr}^e, which controls reactive power of the generator, is determined by the current requirement shown in Fig. 7 corresponding to fault level. Like (33), d-axis rotor- flux command of rotor d-axis (λ_{dr}^*) is determined for tracking the stator flux.

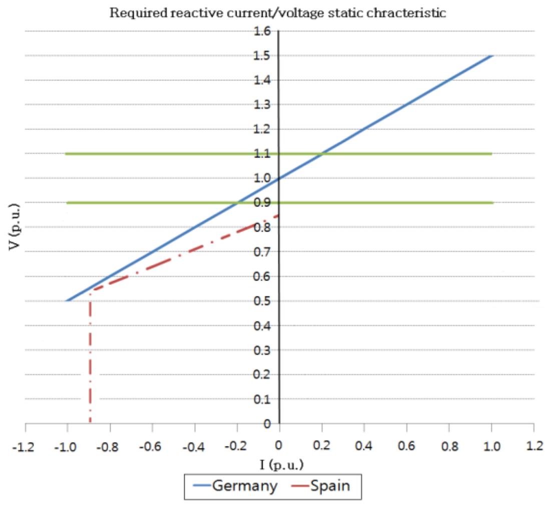

Fig. 7. Reference of reactive output current(ROC) during voltage disturbances, according to the German and Spanish grid codes [13]

$$\lambda_{dr}^* = \lambda_{ds}^e + \sigma L_r I_{dr_{ROC}}^e \tag{33}$$

The flux tracking technique proposed in the paper is shown in Fig. 8. Fig. 9 illustrates the proposed LVRT control block. The υ_{dr-ff}^e and υ_{qr-ff}^e in Fig. 8 and Fig. 9 mean feed-forward terms.

The proposed method protects the system by limiting the over-current of the rotor, but protection scheme provided by hardware is required if the system protections not secured depending on the level of low-voltage [14].

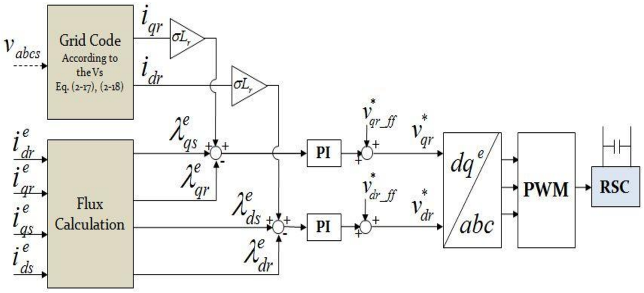

Fig. 8. The proposed flux tracking scheme

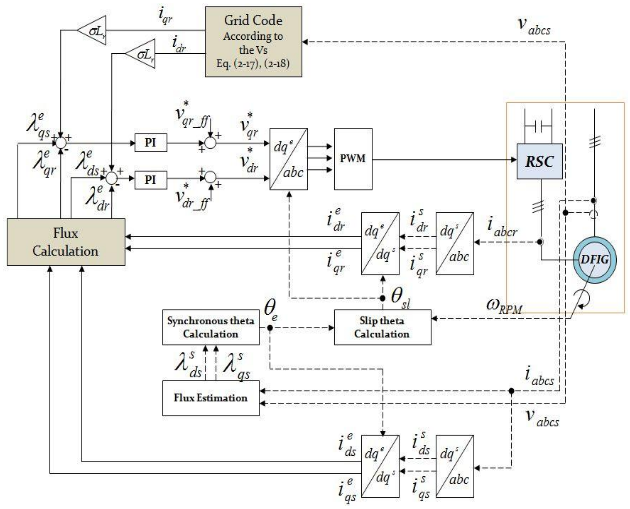

Fig. 9. The proposed LVRT control block diagram

4. Verifications

Fig. 10 shows the grid voltages for simulation studies. This paper coversonly balanced 3-phase low-voltage fault.

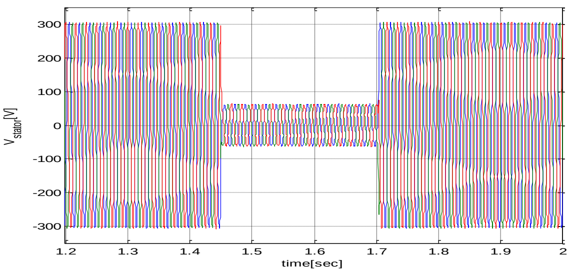

Fig. 10. Stator voltage waveform (The grid voltage)

The fault starts at t=1.43 and has lasted about 0.25 seconds. The level of low-voltage is 20% of the rating voltage. In this paper, due to the large generator inertia and pitch control, the speed of the rotor is assumed almost constant during the fault.

As shown in Fig. 11(a) for without LVRT scheme, the rotor current in low-voltage condition is increased by 2~3 times compared to that in the steady-state condition. Fig. 11(b) confirms that the peak value of rotor current is reduced by the proposed method. Also, reduction of the over-voltage in the DC-link by the proposed method can be known by comparing Figs. 12 (a) and (b), without and with the proposed method, respectively.

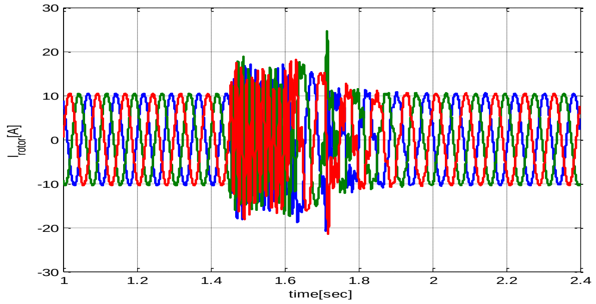

(a)

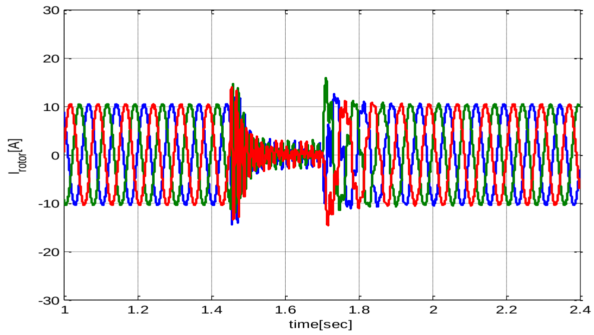

(b)

Fig. 11. Rotor current waveform (a) without and (b) with the proposed method

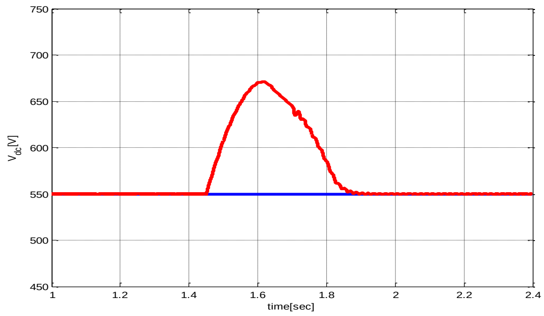

(a)

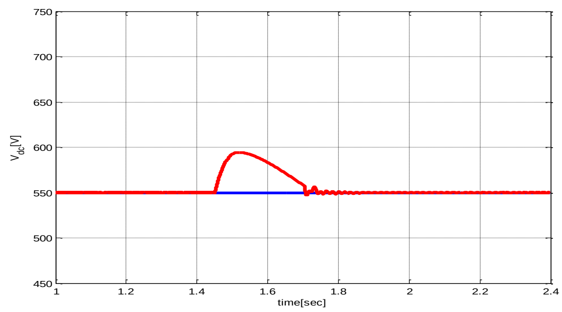

(b)

Fig. 12. DC-link voltage waveform (a) without and (b) with the proposed method

5. Conclusion

This paper proposed a flux tracking LVRT control strategy which protects the over-current of the system by modifying the rotor current commands corresponding to level of voltage dip. The proposed technique is based on system modeling equation in the synchronous rotating reference frame. A rapid and simple fault control can be available by using the value measured in steady-state condition. According to the output waveforms the proposed LVRT control technique is effective against a critical voltage fault. Using computer simulations, the validity of the proposed scheme has been verified

Acknowledgements

This research was supported by Basic Science Research Program through the National Research Foundation of Korea (NRF) funded by the Ministry of Education, Science and Technology (No. 2013 007739)

References

[1] WWEA, 2012 Half-year Report, Oct. 2012.
[2] Brendan Fox, et al., "Wind power integration: connection and system operational aspects," *The Institution of Engineering and Technology*, pp. 53-77, 2007.
[3] B. Singh and S.N. Singh, "Wind power interconnection into the power system: a review of grid code requirements," *The Electricity Journal*, vol. 22, pp. 54-63, June. 2009.
[4] J. Lopez, P. Sanchis, E. Gubia, A. Ursua, L. Marroyo, and X. Roboam, "Control of doubly fed induction generator under symmetrical voltage dips," *ISIE08*, pp. 2456-2462, July. 2008.
[5] K. Lima, A. Luna, P. Rodriguez, E. Watanabe, R. Teodorescu, and F. Blaabjerg, "Doubly-fed induction generator control under voltage sags," *IEEE Energy 2030 Conference*, pp. 1-6, Nov. 2008.
[6] S. Xiao, G. Yang, and H. Zhou, "A LVRT control strategy based on flux tracking for DFIG-based wind power systems," *ICPE&ECCE*, pp. 76-82, 2011.
[7] R. Pena, J.C. Clare, and G.M. Asher, "Doubly fed induction generator using back-to-back PWM converters and its application to variable-speed wind-energy generation," *IEE Proc.-Electr. Power Appl.*, vol. 143, no. 3, pp. 231-241, May. 1996.
[8] O.A. Lara, et al.,"Wind energy generation: modeling and control," *WILEY*, 2009.
[9] I. Erlich, H. Wrede, and C. Feltes, "Dynamic behavior of DFIG-based wind turbines during grid faults," *Power Conversion Conference*, pp. 1195-1200, Apr. 2007.
[10] T.H. Nguyen and D.C. Lee, "Improved LVRT capability and power smoothening of DFIG wind turbine systems," *Journal of Power Electronics*, vol. 11, no. 4, pp. 568-575, July. 2011.
[11] A.O. Ibrahim, T.H. Nguyen, D.C. Lee, and S.C. Kim, "A fault ride-through technique of DFIG wind turbine systems using dynamic voltage restorers," *IEEE Trans. on Energy Conv.*, vol. 26, no. 3, pp. 871-882, Sept. 2011.
[12] Z. Peng and H. Yikang, "Control strategy of an active crowbar for DFIG based wind turbine under grid voltage dips," *ICEMS*, pp. 259-264, Oct. 2007.
[13] M. Tsili, C. Patsiouras, and S. Papathanassiou, "Grid code requirements for large wind farms: a review of technical regulations and available wind turbine technologies," *EWEC*, pp. 1-11, 2008.
[14] C. Wessels and F. W. Fuchs, "Fault ride through of DFIG wind turbines during symmetrical voltage dip with crowbar or stator current feedback solution," *Energy Conv. Congress and Expo.*, pp. 2771-2777, Sept. 2010.

Sun-Young Park received B.S degree in Electronic and Electrical engineering from Hongik University in 2011. She also received M.S degree from Hongik University in 2013. She is currently working as an engineer in LG Electronics HAE R&D Center, Seoul, Korea. Her research interests are motor drives and electric machines.

Hyung-Jin Ahn received B.S degree in Electronic and Electrical engineering from Hongik University. He is currently a M.S. degree student at Hongik University. His research interests are electric machines control and application of renewable energy.

Dong-Myung Lee received his B.S. and M.S. in Electrical Engineering from Hanyang University, Seoul, Korea, in 1994 and 1996, respectively, and his Ph.D. in Electrical and Computer Engineering from the Georgia Institute of Technology, Atlanta, Georgia, USA, in2004. From 1996 to 2000, he worked for LG Electronics Inc., Seoul, Korea. From 2004 to 2007, he was employed by the Samsung SDI R&D Center, Yongin, Korea, as a Senior Engineer. Since 2008, he has been an Associate Professor with the School of Electronic and Electrical Engineering, Hongik University, Seoul, Korea. His current research interests include variable speed drives, power quality compensation devices, and power conversion systems for renewable energy sources.